UC Riverside
UC Riverside Previously Published Works

Title

hPSC-Derived Maturing GABAergic Interneurons Ameliorate Seizures and Abnormal Behavior in Epileptic Mice

Authors

Cunningham, Miles
Cho, Jun-Hyeong
Leung, Amanda
et al.
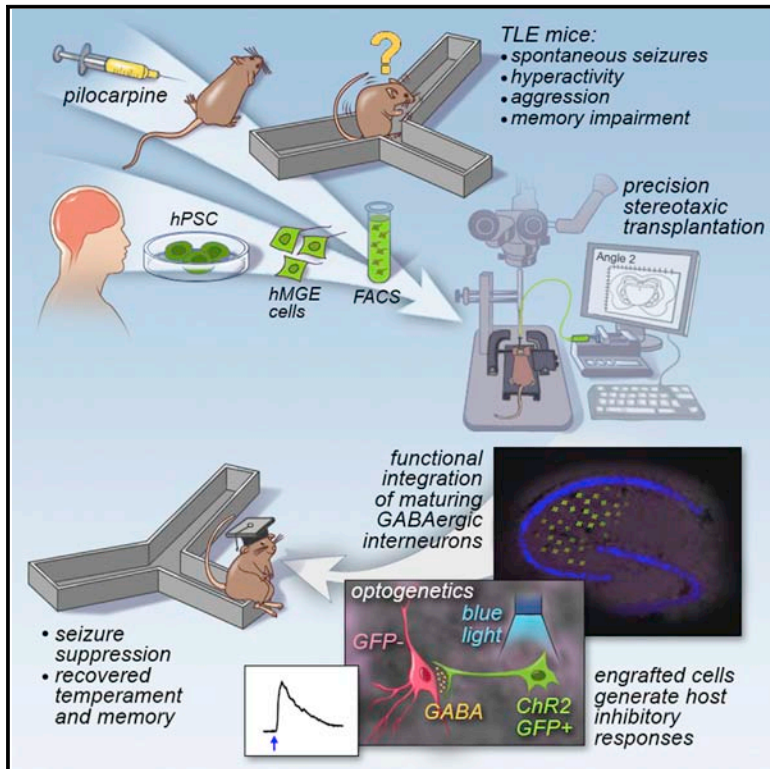
Peer reviewed

Cell Stem Cell

hPSC-Derived Maturing GABAergic Interneurons Ameliorate Seizures and Abnormal Behavior in Epileptic Mice

Graphical Abstract

Highlights

Human-PSC-derived mGINs engraft within mouse epileptic brain

Human mGINs migrate extensively and integrate within host epileptic circuitry

The activation of human mGINs induces inhibitory synaptic responses in host neurons

mGIN grafts suppress seizure and abnormal behavior

Authors

Miles Cunningham, Jun-Hyeong Cho, ...,
Vadim Y. Bolshakov, Sangmi Chung

Correspondence

schung@mclean.harvard.edu

In Brief

In a mouse model of temporal lobe epilepsy, Cunningham et al. use optogenetic approaches to analyze human pluripotent stem cell (hPSC)-derived GABAergic interneurons transplanted into the hippocampus. Engrafted cells suppressed spontaneous seizure activity as well as seizure-associated cognitive deficits, aggressiveness, and hyperactivity.

CrossMark

CellPress

hPSC-Derived Maturing GABAergic Interneurons Ameliorate Seizures and Abnormal Behavior in Epileptic Mice

Miles Cunningham,[3,6] Jun-Hyeong Cho,[4,6,7] Amanda Leung,[1,2] George Savvidis,[1,2] Sandra Ahn,[1,2] Minho Moon,[1,2] Paula K.J. Lee,[1,2] Jason J. Han,[5] Nima Azimi,[3] Kwang-Soo Kim,[1,2] Vadim Y. Bolshakov,[4] and Sangmi Chung[1,2,*]

[1]Molecular Neurobiology Laboratory, Department of Psychiatry and Program in Neuroscience
[2]Harvard Stem Cell Institute
[3]Laboratory for Neural Reconstruction, Department of Psychiatry
[4]Cellular Neurobiology Laboratory, Department of Psychiatry
[5]MRC Electron and Light Microscopy Core Facility
McLean Hospital/Harvard Medical School, Belmont, MA 02478, USA
[6]Co-first author
[7]Present Address: Department of Cell Biology and Neuroscience, University of California, Riverside, Riverside, CA 92521, USA
*Correspondence: schung@mclean.harvard.edu
http://dx.doi.org/10.1016/j.stem.2014.10.006

SUMMARY

Seizure disorders debilitate more than 65,000,000 people worldwide, with temporal lobe epilepsy (TLE) being the most common form. Previous studies have shown that transplantation of GABA-releasing cells results in suppression of seizures in epileptic mice. Derivation of interneurons from human pluripotent stem cells (hPSCs) has been reported, pointing to clinical translation of quality-controlled human cell sources that can enhance inhibitory drive and restore host circuitry. In this study, we demonstrate that hPSC-derived maturing GABAergic interneurons (mGINs) migrate extensively and integrate into dysfunctional circuitry of the epileptic mouse brain. Using optogenetic approaches, we find that grafted mGINs generate inhibitory postsynaptic responses in host hippocampal neurons. Importantly, even before acquiring full electrophysiological maturation, grafted neurons were capable of suppressing seizures and ameliorating behavioral abnormalities such as cognitive deficits, aggressiveness, and hyperactivity. These results provide support for the potential of hPSC-derived mGIN for restorative cell therapy for epilepsy.

INTRODUCTION

Epileptic seizures are characterized by unpredictable abnormal electrical discharge, loss of consciousness, and convulsions, and they are experienced by 1 in 26 individuals at some point in their lifetime (Jensen, 2014). One of the most common forms of seizures is temporal lobe epilepsy (TLE), characterized by epileptic abnormalities in the hippocampus, parahippocampal gyrus, and amygdala (Engel, 2001). About one-third of patients with TLE exhibit intractable seizures that cannot be controlled by antiepileptic drugs (AEDs) (Engel, 2002), and surgical resection of the seizure focus may be necessary (Christoph, 2008). Patients who are not candidates for surgery must live with ongoing seizures—in many cases, multiple events in a single day. Although AEDs can reduce or eliminate seizures for the more fortunate patients, these medicines are associated with diverse and troublesome side effects, including weight gain, metabolic acidosis, hepatotoxicity, movement disorders, and mental status changes (Cramer et al., 2010; Walia et al., 2004). More effective, permanent therapeutic solutions are desperately needed for many of these patients with limited treatment options.

A key pathological feature of human TLE is synaptic reorganization, including neuronal loss and gliosis in CA1 and hilus, granule cell dispersion, and mossy fiber sprouting in the dentate gyrus (Wieser, 2004). Examination of excised epileptic tissue from TLE patients has revealed a loss of interneurons releasing inhibitory neurotransmitter GABA (de Lanerolle et al., 1989; Marco et al., 1996; Spreafico et al., 1998). It is believed that a decrease in GABA-mediated inhibition is a critical contributing factor in epilepsy. Indeed, decreased inhibition has repeatedly been demonstrated in TLE animal models (Cossart et al., 2001; Hirsch et al., 1999; Kobayashi and Buckmaster, 2003). Therefore, one possible therapeutic approach is to increase GABA-mediated inhibition to suppress hyperexcitable neurons during seizure initiation. Early work exploring the potential for inhibitory neural grafts in controlling epileptic activity has shown promise and has inspired further studies (Fine et al., 1990; Lindvall and Björklund, 1992; Löscher et al., 1998). More recent experiments have shown that mouse GABAergic interneuron precursors engrafted into the TLE mouse brain decreased seizure activity (Baraban et al., 2009; Hattiangady et al., 2008; Hunt et al., 2013; Maisano et al., 2012; Southwell et al., 2014).

However, in order to transform such proof-of-principle studies into viable therapeutic approaches for human TLE patients, it is critical to develop optimal human cell sources that can integrate into host circuitry and increase GABA-mediated inhibitory tone, thereby reducing seizure activity in the epileptic brain. Human pluripotent stem cell (hPSC) technologies, including induced PSCs (iPSCs), have the potential to provide an unlimited and

ethically unimpeded source of therapeutic cells (Chen et al., 2014; Mallon et al., 2013; Yu et al., 2013) including human interneurons. Nevertheless, efficient translation of hPSC-derived interneurons could be hampered by their well-known, protracted maturation (Le Magueresse and Monyer, 2013; Nicholas et al., 2013). For example, parvalbumin^{+} neurons acquire fast-spiking properties only after postnatal maturation into early adolescence in mice (Doischer et al., 2008; Okaty et al., 2009).

Using highly efficient methods for generating medial ganglionic eminence (MGE) cells, precursors of maturing GABAergic interneurons (mGINs), from hPSCs (Kim et al., 2014), we transplanted a homogeneous population of human MGE cells into pilocarpine-induced TLE mice, a well-characterized model of human TLE (Curia et al., 2008). Then, we extensively characterized the biology of hPSC-derived mGINs within the epileptic brain. mGINs actively migrate, spreading throughout the entire host hippocampus. Using optogenetic approaches and ultrastructural studies, we demonstrated that grafted mGINs integrate into the dysfunctional host circuitry, receive excitatory inputs, and, in turn, induce inhibitory responses in host neurons by releasing GABA. This ultimately resulted in the reversal of behavioral abnormalities in TLE mice, including spontaneous seizures as well as comorbid cognitive impairment, hyperactivity, and aggressiveness. These findings have compelling implications for the previously undescribed utility of hPSC-derived mGIN to address a desperate need for new therapies for treating seizure disorders.

RESULTS

### Human mGINs Migrate Extensively within the Epileptic Brain

Human MGE cells were generated by in vitro differentiation of H7 human embryonic stem cells according to our optimized procedure (Kim et al., 2014) and purified by fluorescence-activated cell sorting (FACS) with anti-ENCAM prior to transplantation (Figure 1A). Most of the FACS-sorted cells expressed the MGE markers Nkx2.1 and Olig2, as well as the early neural marker nestin, but no cells were positive for the PSC marker SSEA4 (Figure S1 available online). We generated a mouse model for TLE by injecting Nod-Scid mice with 400 mg/kg doses of pilocarpine. Animals demonstrating Racine stage 3–5 seizure activity upon induction with pilocarpine were further screened for occurrence of spontaneous recurrent seizures (SRSs) over 7 days with continuous video monitoring starting 10 days after pilocarpine injection. Mice having at least one SRS during this 7-day screening period were used for further experiments and were denoted as "TLE mice" in this study. Human MGE cells were disseminated throughout most of the hippocampus by depositing volumes of cell suspension within the rostral and caudal hippocampus bilaterally with four separate targets on each side, as reported previously (Hunt et al., 2013) (Figure 1A). Histological analysis showed that, 2 weeks posttransplantation (PT), cells were primarily clustered near the injection site (59,027 ± 18,724 total human nucleus^{+} cells per mouse, n = 3; Figures 1B and 1C). However, at 4 months PT, transplanted mGIN had extensively migrated, becoming well integrated within the host hippocampus (74,913 ± 15,417 total human nucleus^{+} cells per mouse, n = 8; Figures 1D–1J, S2, and S4) without significant dif-

ference in the total surviving cell numbers in comparison to 2 weeks PT (p = 0.58). Stereological analysis demonstrated migration of transplanted human mGIN greater than 1.6 mm from the site of injection (Figure 1K). At 2 weeks PT, most cells expressed GABA and Sox6 as well as Nkx2.1 (Figures 2A–2C), and a minority of cells expressed the more mature neuronal marker NeuN (Figure 2E). However, at 4 months PT, the majority of cells expressed NeuN and β-tubulin as well as GABA and Sox6 (Figures 2G, 2H, 2J, and 2R–2T). The expression of precursor marker Nkx2.1 was significantly diminished at 4 months PT in comparison to 2 weeks PT (Figures 2I and 2W), whereas the mature interneuron marker Lhx6 was significantly increased at 4 months PT in comparison to 2 weeks PT (Figures 2D, 2K, and 2W). In addition, proliferating cell marker Ki67 was significantly decreased after 4 months PT in comparison to 2 weeks PT (Figures 2F, 2L, and 2W). Furthermore, at 4 months PT, some GABAergic interneurons were found to express somatostatin, parvalbumin, calretinin, neuropeptide Y, and calbindin (Figures 2M–2Q, 2X, and S5A–S5F). As seen during in vivo embryonic development, interneuron maturation was not synchronous, and cells with simple bipolar morphology and cells with more complex neurites coexist at this time point (Figure S5G–S5L). Transplanted cells generated very small numbers of astrocytes (GFAP[+]; Figures 2U and 2X) or oligodendrocyte lineage cells (Olig2^{+}; Figures 2V and 2X).

Functional Integration of Human mGINs into the Epileptic Brain

Electrophysiological and morphological analyses were used to determine whether transplanted human MGE cells develop into functional GABAergic neurons and integrate into host neural circuitry. Human MGE cells, transduced with lentivirus in order to stably express channelrhodopsin-2 (ChR2) (H134R)-GFP fusion under a synapsin promoter, were transplanted into the hippocampus of TLE mice. Then, 2 to 5 months after transplantation, grafted human-MGE-derived cells were identified with green fluorescence in acute brain slices containing the hippocampus (GFP^{+} cells; Figure 3A). All 31 GFP^{+} cells displayed typical ChR2-mediated currents induced by blue light illumination (Figure 3B), indicating that recorded GFP^{+} cells were indeed human-MGE-derived cells expressing ChR2. Consistently, short pulses of blue light illumination evoked action potential (AP) firings in most GFP^{+} cells (Figure 3C), suggesting that grafted GFP^{+} cells can be activated by photostimulation in brain slice preparations. Passive membrane properties of GFP[+] human mGINs, including resting membrane potential (RMP) and membrane resistance (R_m), were similar to those reported previously (Nicholas et al., 2013) (Figure 3D). However, unlike the previous report, we did not observe an increasing trend of the membrane capacitance (C_m) of the grafted cells (Figure 3D). This discrepancy may be due to the different experimental conditions that human MGE cells were transplanted into the brain in our study, whereas they were grown in culture in the previous report. Thus, our findings reflect the membrane properties of human MGE cells under more physiological conditions. In comparison to host hippocampal interneurons in adult mice, RMP was significantly depolarized in grafted mGIN (Figure 3D; p < 0.001), suggesting that grafted cells were not fully mature at this time point. However, there was no significant difference in R_m and C_m between human
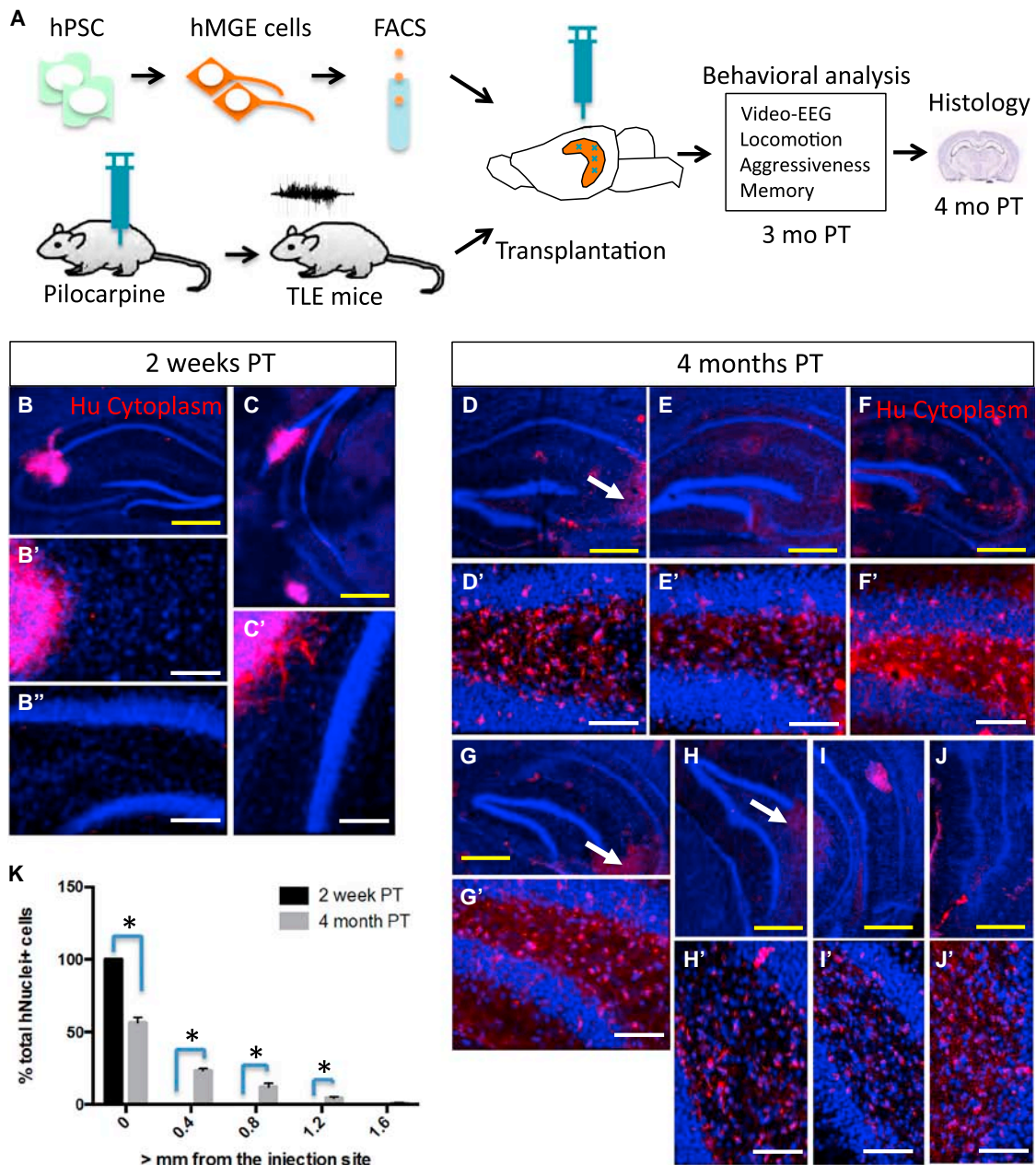
Figure 1. Transplanted Human mGIN Migrate Robustly and Integrate in Adult Epileptic Brain
(A) Overall experimental design. hPSC-derived MGE cells were transplanted into the hippocampus of TLE mice. Behavioral analysis was conducted after 3 months PT and histology analysis at 4 months PT.
(B–C) Two weeks PT, transplanted cells display minimal migration, shown by human cytoplasm-specific antibody staining (B', B," and C' show enlarged photomicrographs of dentate gyrus regions from corresponding pictures).
(D–J) Four months PT, transplanted cells display robust migration and integration into the host brain, as shown by human cytoplasm-specific antibodies (D'–J' show enlarged photomicrographs of dentate gyrus regions from corresponding pictures, depicting migration from the injection site). White arrows indicate injection sites. Yellow scale bars represent 500 μm. White scale bars represent 100 μm.
(K) Quantification of migration of transplanted cells (mean ± S.E.M.; *p < 0.05, two tailed Student's t test) 2 weeks PT (n = 3) and 4 months PT (n = 8).
See also Figures S1–S4

mGINs versus host interneurons. When voltage pulses were applied, grafted human mGINs showed rapidly desensitizing inward currents activated at membrane potential > –40 mV (Figure 3E), indicating the expression of voltage-gated Na^+ channels. In current-clamp mode, 45% of human mGINs displayed spontaneous AP firings at resting membrane potential at 2.0 ± 0.2 Hz (Figures 3F and 3G), suggesting that some of the grafted mGINs generate tonic firings.
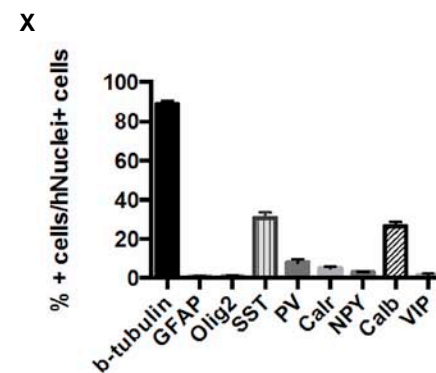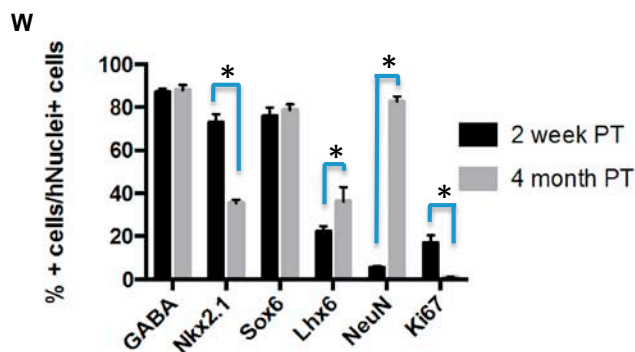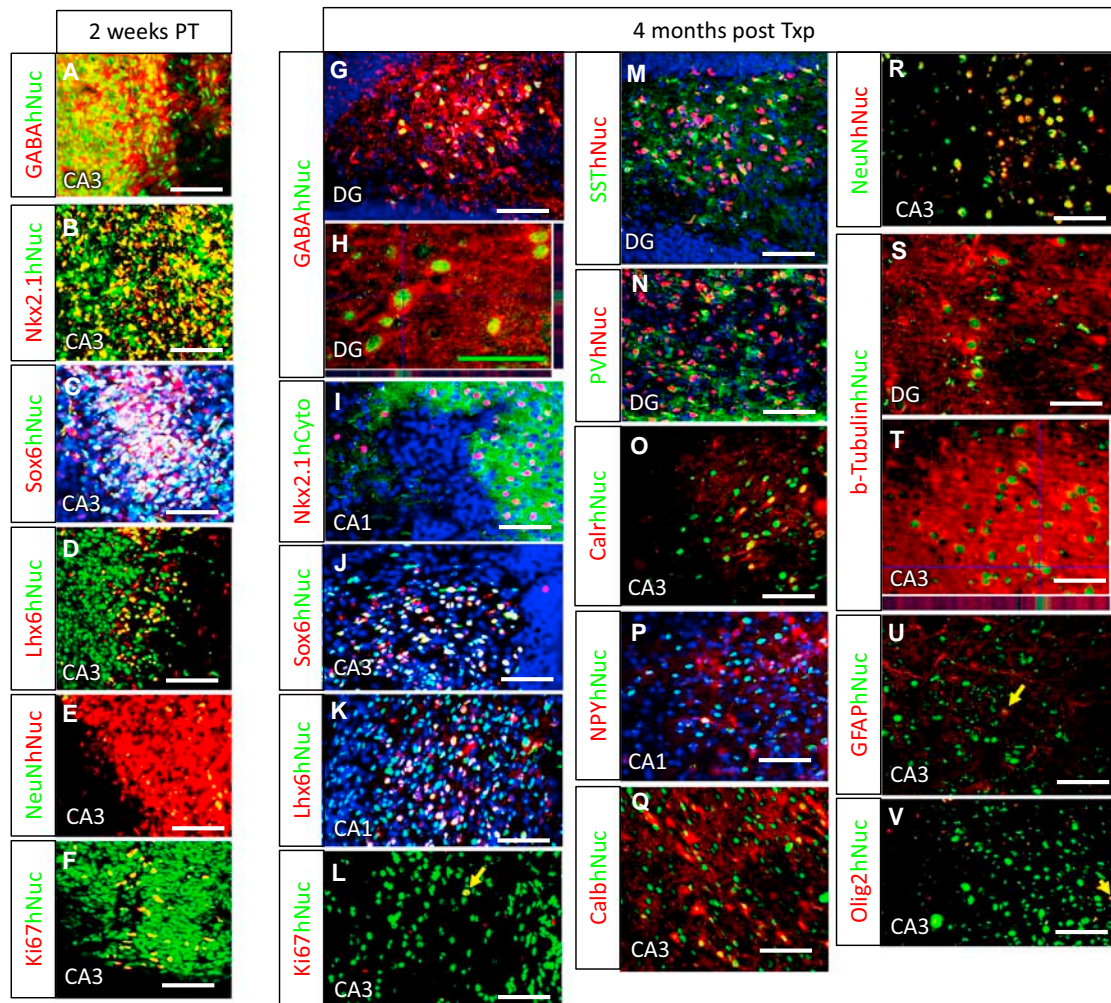
Figure 2. Transplanted Human MGE Cells Generate mGIN in Adult Epileptic Brains
(A–F) Immunohistochemical analysis of transplanted cells 2 weeks PT.
(G–V) Immunohistochemical analysis of transplanted cells 4 months PT. SST, somatostatin; PV, parvalbumin; Calr, calreticulin; NPY, neuropeptide Y; Calb, calbindin. Green scale bar represents 50 μm. White scale bars represent 100 μm.
(W) Cell-counting analysis of 2 weeks PT versus 4 months PT (mean ± SEM; n = 3, *p < 0.05, two tailed Student's t test).
(X) Cell-counting analysis at 4 months PT (n = 3).
See also Figure S5.

Furthermore, the injection of depolarizing currents induced AP firings in all human mGINs examined (Figures 4A and 4B). As for passive membrane properties, grafted mGINs displayed less

mature biophysical properties of AP firings in comparison to the host interneurons in terms of posthyperpolarization and AP width (Figure 4B), consistent with their well-known protracted
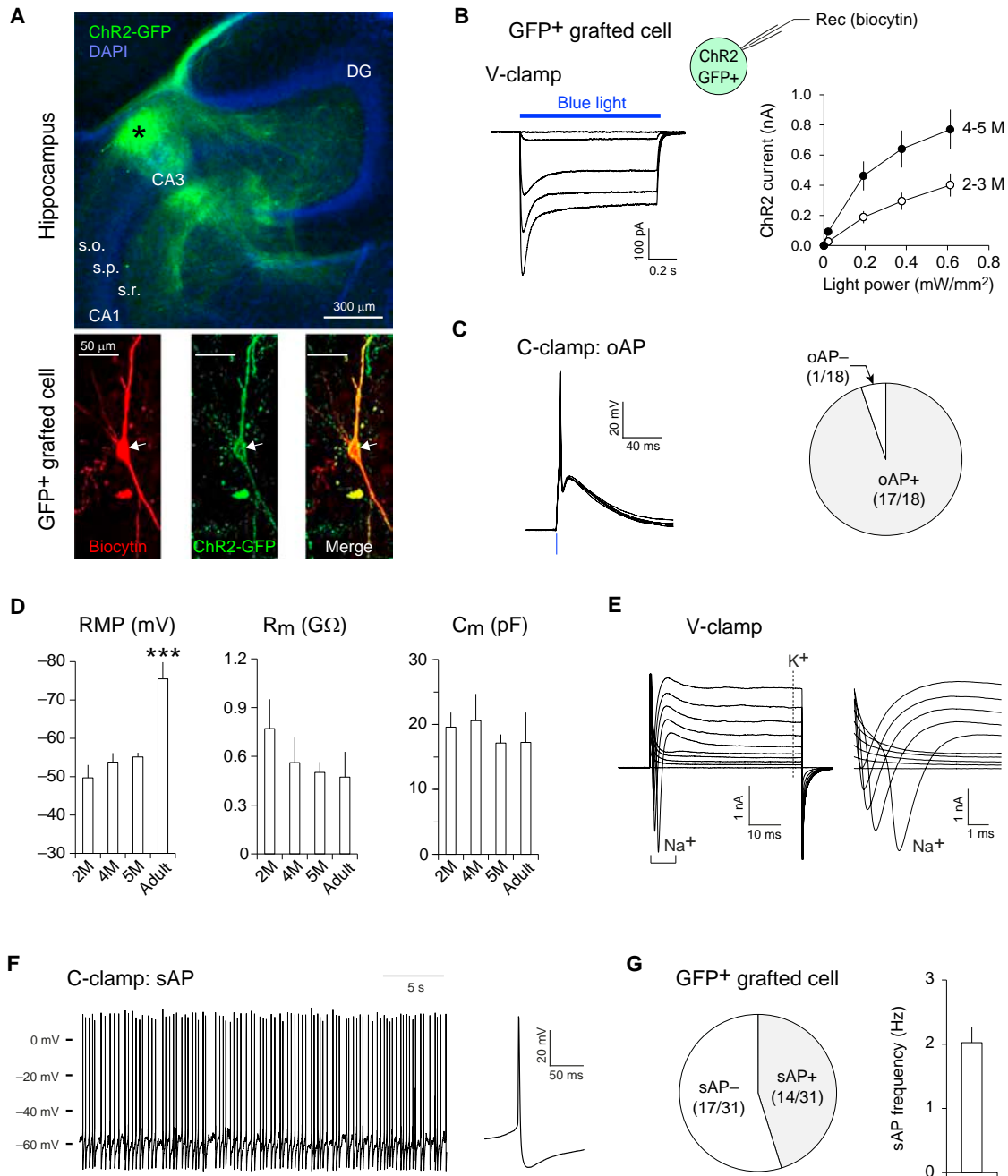
Figure 3. Electrophysiological Characterization of Grafted Human mGIN in the Hippocampus

(A) Top, a microscopic image showing the distribution of grafted human mGIN in the hippocampus. Channelrhodopsin 2 (ChR2)/GFP-expressing human MGE cells (green) transplanted into the cornu ammonis region 3 (CA3) of the hippocampus migrate extensively to the CA1 and dentate gyrus (DG). The graft core is indicated by an asterisk. Strata oriens (s.o.), pyramidale (s.p.), and radiatum (s.r.) are also indicated. Bottom, confocal microscopic images showing that the recorded grafted cell labeled with biocytin-streptavidin (red, left) expresses ChR2-GFP (green, middle).

(B) Whole-cell patch-clamp recordings were performed with grafted cells expressing ChR2-GFP. Grafted human mGIN were identified with green fluorescence in acute brain slices. Biocytin was included in the pipette solution to label the recorded cells. Left, representative traces of ChR2-mediated currents in a grafted cell. These inward currents were induced by blue light illuminations (470 nm, 1 s pulses, blue horizontal bar) with variable intensities (0.02–0.61 mW/mm^2) and recorded at –80 mV in voltage-clamp (V-clamp) mode. Right, a summary graph showing the peak amplitude of ChR2-mediated currents plotted versus light power. ChR2 currents were larger in human mGIN 4–5 months after transplantation (n = 16 cells) than in cells 2–3 months after implantation (n = 9 cells; p < 0.001).

(C) Representative traces of AP evoked by short pulses of blue light illumination (1 ms, 12.5 mW/mm^2, blue vertical line, left). These optogenetically-induced APs (oAPs) were recorded in current-clamp (C-clamp) mode at approximate –85 mV and were detected in most grafted human mGIN examined (n = 18 cells, right).

(D) Summary plots of resting membrane potential (RMP), membrane resistance (R$_m$), and a fast component of membrane capacitance (C$_m$) of grafted human mGINs, which were examined 2, 4, or 5 months after transplantation (n = 6, 8, and 11 cells, respectively) as well as host adult hippocampal interneurons (adult, > 3 months old, n = 4 cells). ***p < 0.001, adult versus all other groups.

maturation (Nicholas et al., 2013), whereas there was no significant difference in AP threshold. When grouped based on AP firing, most human mGINs displayed repetitive (type A, 52%) or single AP firing (type B, 32%), whereas delayed (13%) or burst firing pattern (3%) was also observed in a small proportion of transplanted cells (Figure 4C). Furthermore, although more frequent AP firings were induced by small current injections (<50 pA) in repetitive-firing type A cells, type B cells generated only one to three AP firings induced by much larger current injections (>50 pA; Figure 4E). As expected, R_m was significantly larger in type A cells than type B cells (Figure 4E), accounting for different firing patterns of these cells.

After recording, we collected the intracellular contents of the recorded cells and performed single-cell RT-PCR in order to examine the RNA profile of transplanted human mGINs (Figure 4F). Most grafted cells expressed glutamate decarboxylase (GAD) and Sox6, whereas some grafted cells also expressed other GABAergic neuronal markers including parvalbumin, calreticulin, somatostatin, vasoactive intestinal peptide, and neuropeptide Y (Figure 4G). We also performed morphological analysis with biocytin-labeled human mGINs and found characteristic neuronal morphologies with various patterns of neuronal processes (Figure S6). Therefore, these results demonstrate that transplanted human MGE cells develop into mGIN with diverse electrophysiological, biochemical, and morphological properties in the epileptic hippocampus.

Then, we investigated whether grafted human mGIN possessed functional postsynaptic mechanisms allowing synaptic transmission from host neurons. Using confocal microscopic imaging, we observed postsynaptic dendritic spines in biocytin-labeled grafted cells, suggesting that they may receive excitatory synaptic inputs (Figures 5A and 5B). Consistently, in acute hippocampal slices, two-thirds of 21 GFP+ mGINs showed spontaneous postsynaptic currents at –85 mV in voltage-clamp mode at a frequency > 0.1 Hz (Figures 5C and 5E). Moreover, these currents were inhibited completely by NBQX, an AMPA/kainite-type glutamate receptor antagonist (Figure 5D), indicating that they were mediated by excitatory neurotransmitter glutamate. There were no significant differences in biophysical properties of spontaneous postsynaptic activities between grafted human mGINs and host hippocampal interneurons (Figures 5F–5I). These results suggest that most human mGINs transplanted into the hippocampus have functional postsynaptic machinery and receive excitatory synaptic inputs from host glutamatergic neurons. Immunocytochemistry analysis also showed that many postsynaptic PSD95+ puncta on GFP+ grafted cells were juxtaposed with presynaptic synaptophysin puncta (Figure 5J; 2.18 ± 0.56 PSD95+ puncta per 10 μm GFP+ dendrite, n = 22 dendrite segments), suggesting the formation of host glutamatergic synapses onto transplanted human mGINs. Further confirmation of func-

tional synapse formation between host and transplanted neurons was obtained from ultrastructural analysis by transmission electron microscopy (TEM). Examination of hippocampal areas in brain slices immunostained with diaminobenzidine (DAB) for human cytoplasm (human cytoplasm+) showed synaptic connections onto grafted mGINs (Figures 5K–5L). These combined electrophysiological and ultrastructural data demonstrate functional synaptic integration of grafted mGINs into host parenchyma.

Activation of Human mGINs Induces GABA-Mediated Inhibitory Postsynaptic Responses in Host Hippocampal Neurons

Next, we investigated whether grafted human mGINs also have functional presynaptic machinery to release GABA and induce inhibitory postsynaptic responses in host hippocampal neurons (Figure 6A). To this end, we used optogenetic approaches to selectively stimulate ChR2-expressing transplanted cells in hippocampal slices (Figure 6B). Blue light illumination induced ChR2-mediated inward current and AP firings in GFP+ grafted cells (Figures 3B and 3C), whereas the same photostimulation did not induce such currents in any GFP– cells tested (Figure 6B), suggesting that grafted cells can be selectively activated in acute brain slices with this approach. Under these conditions, short pulses of photostimulation, activating ChR2-expressing grafted cells, induced postsynaptic responses in 44% of a total 27 GFP– cells (Figures 6C and 6D). The recorded postsynaptic currents showed a short synaptic delay, indicating monosynaptic origin (Cho et al., 2013). Furthermore, these synaptic responses were inhibited completely by bicuculline, a GABA$_A$ receptor antagonist (Figures 6C and 6D), suggesting that they were mediated by inhibitory neurotransmitter GABA. The current-voltage relationship revealed the reversal potential of these currents at –70 ± 3 mV (Figure 6E), consistent with the estimated reversal potential of chloride ion (–65 mV under our experimental conditions). In some GFP– cells, photostimulation induced probabilistic quantal responses (Figures 6F and 6G), confirming their synaptic nature. Moreover, train photostimulation at 1 Hz induced postsynaptic responses without significant reduction in peak amplitude (Figure 6H and 6I), suggesting that the repetitive activation of grafted mGIN can consistently induce GABAergic responses in GFP– cells. Considering that grafted cells constitutes 30.7% ± 4.7% of total cells at the graft core (n = 6 mice), where the density of GFP+ cells is highest, and that 26.3% ± 4.7% of grafted cells are GFP+, the majority of the recorded GFP– cells would be host hippocampal neurons. Thus, our results suggest that the activation of transplanted human MGE-derived cells can generate inhibitory postsynaptic responses in host hippocampal neurons.

Imaging studies provided additional evidence for the formation of inhibitory synaptic connections onto host neurons by

---

(E) Representative traces showing currents induced by voltage pulses in a grafted cells. Membrane potential was held at –85 mV in voltage-clamp mode. Left, square voltage pulses from –85 to 5 mV with increment of 10 mV (50 ms long) induced both transient inward (Na+, a bracket) and sustained outward currents (K+, a vertical dotted line), which are likely to be mediated by voltage-gated Na+ and K+ channels, respectively. Right, the same trace was zoomed in to visualize the transient inward currents mediated by voltage-gated Na+ channels.

(F) A representative trace of spontaneous AP firings (sAP) in a grafted human mGINs. AP firings were recorded at RMP in current-clamp mode without current injection or withdrawal. A trace on the right is the average of sAP recorded in the same neuron.

(G) Left, spontaneous sAPs were detected at RMP in 45% of total 31 grafted cells examined. Right, a summary graph showing the average frequency of sAPs (n = 14 cells). Error bars are SEM.
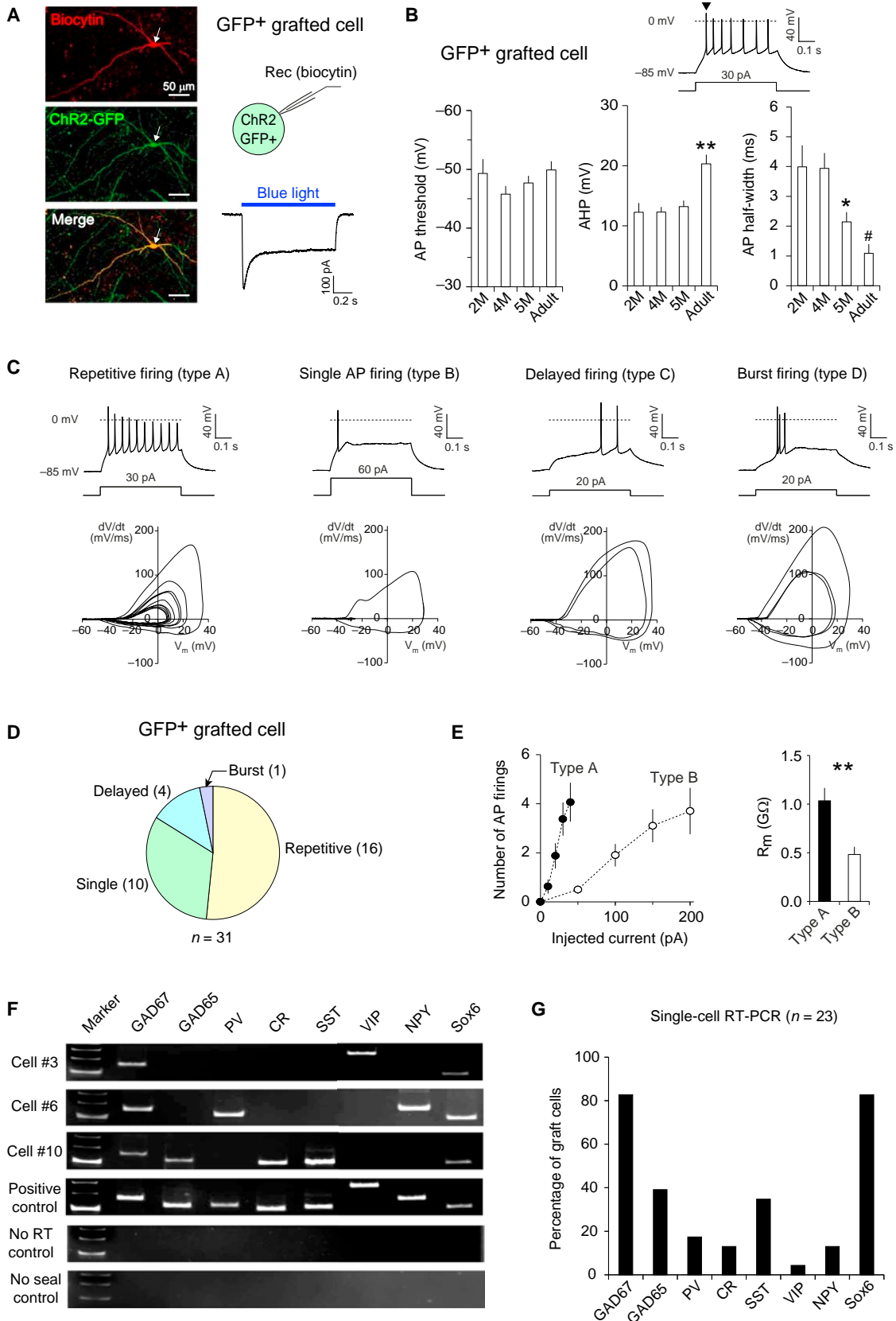
(legend on next page)

transplanted human mGINs. Fluorescence microscopy showed that many of the presynaptic VGAT+ puncta on GFP+ mGINs were juxtaposed with postsynaptic gephyrin+ puncta (Figure 6J). TEM ultrastructural studies also identified symmetric synaptic contacts between presynaptic grafted cells and postsynaptic host neurons (Figures 6K and 6L). These combined results suggest that grafted human mGIN have presynaptic machinery for releasing GABA and inhibiting host hippocampal neurons as well as postsynaptic machinery for receiving excitatory inputs from host neurons.

Human mGINs Reduce Seizure Activity in Epileptic Mice and Ameliorate Behavioral Abnormalities

Our electrophysiological findings suggest that transplanted human mGINs integrate into host hippocampal circuitry and may be sufficient for exerting antiepileptic effects by releasing inhibitory neurotransmitter GABA and increasing inhibitory synaptic responses in host hippocampal neurons. Therefore, we next investigated the therapeutic potential of transplanted human mGINs for preventing seizures in our TLE mouse model. Seizure activity of engrafted TLE mice was analyzed 3 months after transplantation by continuous electroencephalography (EEG) video monitoring. Vehicle-injected control TLE mice with sham surgery (n = 11) showed seizure EEG activity with high-frequency and high-voltage synchronized polyspikes (Figure 7A) and had a seizure event frequency of 1.92 ± 0.45 seizures per day. However, mGIN-grafted TLE mice (n = 9) showed significantly reduced seizure event frequency (0.13 ± 0.07 seizure per day); in five animals in this group, seizure activity was eliminated entirely (Figure 7A). Seizure EEG activity was confirmed by simultaneous video recording, which showed clonus and rearing and falling of the mice (Racine stages 3–5; Movie S1). Naive Nod-Scid mice without pilocarpine injection did not show any seizure EEG activity during the monitoring (n = 6). The duration of seizures was not significantly different between control TLE mice

and mGIN-grafted TLE mice (39 ± 2.7 s versus 42.8 ± 8.7 s, n = 4–10, p = 0.61). These results indicate that transplantation of human mGINs suppresses seizure activity in the TLE mouse model.

Because epilepsy patients frequently suffer from comorbid cognitive impairment and psychiatric symptoms (Brooks-Kayal et al., 2013), we next analyzed the effect of human mGIN transplantation on other behavioral abnormalities of TLE mice. Previous studies have shown that these animals, similar to TLE patients, show cognitive deficits (Gröticke et al., 2007), which could be reversed by engrafting mouse fetal MGE cells (Hunt et al., 2013). Therefore, we tested whether transplanted mGIN can improve cognitive function of TLE mice in a similar manner. In a Y maze test, control TLE mice (n = 10) showed significant deficits in short-term working memory in comparison to naive mice (n = 9). This deficit was abolished after mGIN transplantation (n = 8), whereas there was no significant difference in total arm entry among test groups (p = 0.49, Figure 7B). In novel object recognition test, an independent measure of learning and memory, control TLE mice (n = 11) showed significantly decreased time exploring the novel object in comparison to the naive mice (n = 12), whereas this deficit was reversed after mGIN transplantation (n = 8; Figure 7C). The frequency of novel object exploration showed a similar trend as the duration of novel object exploration but did not reach statistical significance (p = 0.19). These data suggest that transplantation of human mGINs can reduce cognitive deficits in rodent model of TLE.

In addition to cognitive deficits, hyperactivity and aggressiveness have been reported in the pilocarpine-induced rodent model of TLE (Müller et al., 2009; Rice et al., 1998). Consistently, control TLE mice (n = 11) displayed significantly higher locomotor activity in comparison to the naive mice (n = 14), as measured with a photobeam activity system (PAS). However, animals engrafted with human mGINs displayed a significant attenuation of this abnormality (n = 8; Figure 7D). Moreover, hypervigilance

Figure 4. Transplanted Human MGE Cells Differentiate into GABAergic Interneurons in the Epileptic Hippocampus

(A) Left, microscopic images of a recorded human MGE cell in acute hippocampal slices. ChR2/GFP-expressing human MGE cells were identified with green fluorescence and labeled with biocytin-streptavidin (red) with recording pipettes. Right, blue light illumination (470 nm, 0.61 mW/mm^2, blue horizontal bar) induces ChR2-mediated currents recorded at –80 mV in voltage-clamp mode, confirming that the recorded cell is a grafted cell.

(B) Analysis of AP firings in human mGIN transplanted into the hippocampus. Top, a representative trace of AP firings in a ChR2/GFP-expressing grafted cell. APs were induced by depolarizing current injection near threshold (500 ms long) and recorded in current-clamp mode at approximate –85 mV. The amount of injected currents is indicated below the trace. For each grafted cell, the first AP (an arrowhead) was analyzed. Bottom, summary graphs showing the average AP threshold (left), afterhyperpolarization (AHP, middle), and AP half-width (right) in human mGIN examined 2, 4, and 5 months after transplantation (n = 6, 8, and 11 cells, respectively) as well as host adult hippocampal interneurons (adult, > 3 months old, n = 4 cells). **p < 0.01, adult versus all other groups; *p < 0.05, 5 month versus 4 month group; #p < 0.05, adult versus 2 or 4 month group.

(C) Representative traces (top row) and phase plots (bottom row) of four different types of AP firings recorded in grafted human mGINs in hippocampal slices. APs were induced by near-threshold depolarizing current injections in GFP+ grafted cells and were recorded as in (B). Most grafted cells displayed either repetitive firings (type A, first column) or single AP firing (type B, second column) while delayed (type C, third column) or burst firing patterns (type D, fourth column) were observed in a small proportion of grafted cells. Repetitive AP firings could be induced by small current injections in type A cells (<50 pA), whereas type B cells fires only a few APs, which required relatively larger current injections (>50 pA). The amount of injected currents is indicated below the traces. Baseline membrane potential was approximately –85 mV.

(D) A summary graph showing the proportion of grafted human-MGE-derived cells displaying four different AP firing patterns (n = 31 cells).

(E) Left, a summary plot of AP firings in human mGIN in the hippocampus. The number of AP firings was plotted versus injected currents (500 ms long). Note more frequent AP firings induced by small current injections in type A cells (n = 16 cells) than type B cells (n = 10 cells). Right, the average membrane resistance (R_m) in type A was larger significantly than type B cells. **p < 0.01. Error bars are SEM.

(F) Examples of RNA profiles of three grafted cells from single-cell RT-PCR (scRT-PCR, top three rows). Intracellular contents of grafted cells were harvested individually after whole-cell patch-clamp recordings. Positive control with total RNA from the human brain as well as two negative controls (no RT control and no giga-seal formation) are also included in middle and bottom rows. M, size marker (300, 200, and100 bp from top to bottom). PV, parvalbumin; CR, calreticulin; SST, somatostatin; VIP, vasoactive intestinal peptide; NPY, neuropeptide Y.

(G) A summary plot of RNA profile of grafted human mGIN from scRT-PCR (n = 23 cells). Error bars represent SEM.

See also Figure S6.
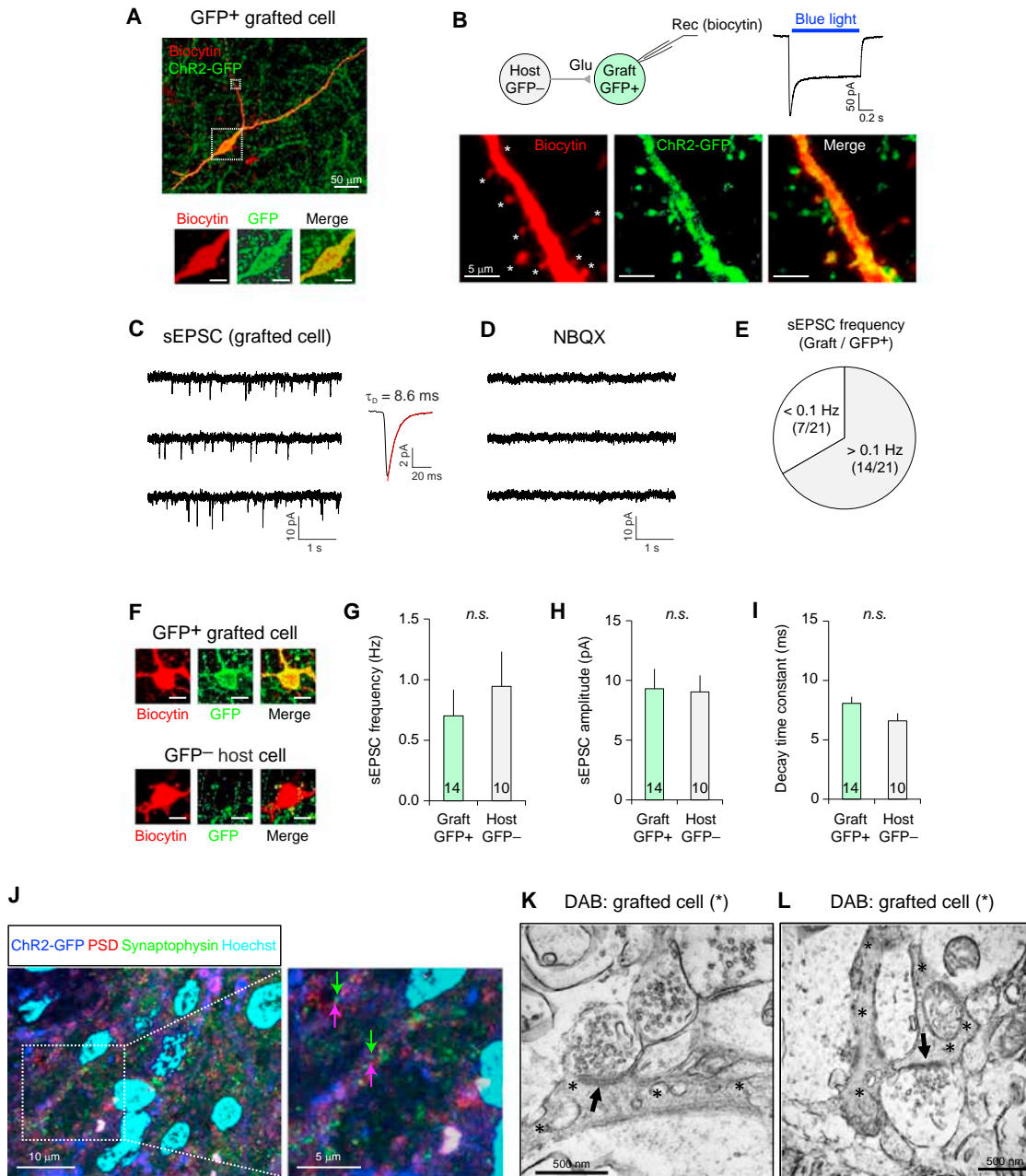
Figure 5. Transplanted Human mGIN Receive Glutamatergic Inputs from Host Neurons

(A) A representative image of a human mGINs transplanted into the hippocampus (green). The ChR2/GFP-expressing grafted cell was labeled with biocytin with a recording patch pipette (red). The cell body is indicated as a larger dotted square and is zoomed in below the image. Scale bar represents 20 μm.

(B) Top left, grafted human mGINs were recorded in acute brain slices. Grafted cells, identified with green fluorescence, receive synaptic inputs from host neurons. The recorded cell was labeled with biocytin-streptavidin (red) using patch pipettes. Top right, blue light illumination induced inward currents, confirming that the recorded cell is a grafted cell expressing ChR2-GFP. ChR2-mediated currents were induced and recorded as in Figure 4A. Bottom, confocal microscopic images show a portion of dendrites of the recorded human mGIN and are the zoomed-in images of that indicated as a smaller dotted square in (A). Dendritic spines are indicated by asterisks.

(C) Left, a representative trace of postsynaptic responses recorded in a GFP+ grafted cell. Spontaneous excitatory postsynaptic currents (sEPSCs) were recorded in GFP+ grafted cells at −85 mV in voltage-clamp mode. Right, a trace showing the average of sEPSCs recorded in the same cell. Decay time constant (τ_D) of sEPSC was calculated by fitting the decay phase of the trace to a single exponential function (red curve).

(D) The application of 10 μM NBQX inhibited sEPSC completely in the same grafted cell as in (C), indicating that sEPSCs were mediated by AMPA/kainate-type glutamate receptors and that the grafted cell receives functional synaptic inputs from host glutamatergic neurons. n = 4 cells.

(E) Two-thirds of recorded human mGINs displayed spontaneous postsynaptic responses with the frequency > 0.1 Hz.

(F) Representative images of the cell bodies of GFP+ grafted cells (top) and GFP− host hippocampal interneurons (bottom). The recorded cells were labeled with biocytin-streptavidin (red) as in (A). Scale bar represents 20 μm.

(legend continued on next page)

and aggressiveness normally observed in control TLE mice (n = 11) were completely reversed to levels of naive mice (n = 15) after transplantation of human mGINs (n = 10; Figure 7E and Movie S2). In sum, these results suggest that transplantation of human mGINs suppresses seizure activity in epileptic mice and ameliorates other behavioral abnormalities.

DISCUSSION

Although fetal MGE cell transplantation has demonstrated proof of principle for cell-based therapy of epilepsy (Hattiangady et al., 2008; Hunt et al., 2013), clinical application is limited by the lack of standardized and reliable cell sources as well as ethical controversies associated with using fetal cells. hPSC technology offers the potential to provide cell sources that are well-characterized, quality-controlled, and virtually unlimited in supply, so long as efficacious progenies can be proficiently derived. We have utilized optimized differentiation of human PSCs into MGE cells (Kim et al., 2014) and report functional efficacy of mGIN in order to reduce epileptic activity and comorbid behavioral abnormalities in the epileptic brain even before they attain full maturity. Considering full electrophysiological maturation of human GABAergic interneurons could take years (Le Maguer-esse and Monyer, 2013; Nicholas et al., 2013), our findings with human mGINs provide a major step toward developing an efficient and cell-based therapy for treating intractable epilepsy.

We have demonstrated that PSC-derived human mGINs migrate extensively within the epileptic hippocampus, integrate into host circuitry and reduce seizure activity and other behavioral abnormalities. The primary mechanisms of the functional effects of grafted mGINs are suggested by our electrophysiological studies. Although they are not fully mature, approximately half of transplanted human mGINs fire spontaneous APs at ~2 Hz, indicating that they are tonically active even without extrinsic synaptic inputs. Moreover, transplanted human mGINs fully integrate into the hippocampal circuitry, receiving excitatory synaptic inputs from host glutamatergic neurons, and are therefore activated by host signals. In turn, our optogenetic studies revealed that grafted human mGINs release inhibitory neurotransmitter GABA in an activity-dependent manner. Therefore, the activation of transplanted mGINs, either by spontaneous activity or by excitatory synaptic drive, causes an increase of inhibitory synaptic responses in host hippocampal neurons, shifting excitation/inhibition balance toward inhibition and suppressing exaggerated neural activity in the epileptic brain. Consistent with previous work (Hunt et al., 2013), we did not observe significant changes in mossy fiber sprouting by human MGE transplantation in comparison to control TLE mice (Figure S7), suggesting that regulation of inhibitory balance alone by grafted cells may be sufficient to exert the antiepileptic effects observed in this study.

Cell therapy for epilepsy offers a number of advantages over conventional therapies. Distinct cell types can be precisely engrafted into brain substructures (Bjarkam et al., 2010), averting the acute and long-term systemic adverse effects seen with AEDs. Furthermore, neural grafts, with their ability to integrate within the host circuitry, would circumvent the need for daily dosing and sluggish titration required with AED administration. A self-regulating therapeutic system of mGIN grafts would eliminate the need of carrying devices to monitor and control seizures. Temporal lobectomy has been used as a last-resort intervention for intractable epilepsy but is associated with surgical morbidity and permanent dysfunction. However, high-precision stereotactic engraftment of stem cells is less invasive and leaves functional neural tissue undisturbed.

Here, we have demonstrated the biology and utility of hPSC-derived mGIN to ameliorate the symptoms of a prevalent and debilitating neuropsychiatric disease. While the efficacy of mouse fetal interneurons to ameliorate seizure activity has been demonstrated previously (Baraban et al., 2009; Hattiangady et al., 2008; Hunt et al., 2013; Maisano et al., 2012; Southwell et al., 2014), the current investigation is the first to demonstrate the therapeutic efficacy of hPSC-derived interneurons to treat epilepsy, and it represents the potential for a reliable and ethically unimpeded cell source for this purpose. Before transition into the clinic setting, however, the question of 'dosing' of MGE cell grafts will need to be addressed. Interestingly, it has been reported that an increase in inhibition reaches a plateau with relatively low numbers of transplanted interneurons (Southwell et al., 2010). This suggests that larger numbers of interneurons are unlikely to result in adverse effects, but at the same time, smaller, less-intrusive deposits of cells may produce an optimal response. In addition, further evaluation of long-term graft survival and safety should be assessed before undertaking clinical applications. Porcine human simulation neurosurgery is presently underway to establish such criteria prior to human trials (M.C., unpublished data). In addition, isolation, and purification of cortical interneuron populations with appropriate cell-surface markers will facilitate the generation of quality-controlled cell sources for human trials. With prudent preclinical testing, this technology holds promise as a therapeutic approach for TLE as well as other intractable diseases of the CNS.

EXPERIMENTAL PROCEDURES

#### PSC Culture and Differentiation into MGE Cells

H7 hPSCs were maintained and differentiated into MGE cells as described previously (Kim et al., 2014). Differentiated MGE cells were subject to FACS after staining with anti-ENCAM (BD Biosciences) prior to transplantation. Detailed information can be found in the Supplemental Experimental Procedures.

(G–I) Summary plots of the frequency (G), peak amplitude (H), and decay time constant (I) of sEPSC recorded in GFP$^+$ grafted cells (n = 14) and GFP$^-$ host hippocampal interneurons (n = 10). No significant difference was detected between grafted and host cells (n.s.).

(J) A representative image of immunohistochemistry analysis of human mGINs transplanted in the hippocampus. Hoechst (sky blue) was used as nuclear counterstain. Arrows in magenta indicate postsynaptic densities of GFP$^+$ grafted cells (double-stained with ChR2-GFP and PSD), and green arrows indicate presynaptic axon terminals (stained with synaptophysin, green) of GFP$^-$ cells.

(K and L) TEM images showing that grafted human mGIN receive synaptic inputs from host cells. Transplanted cells, stained with DAB for human-cytoplasm-specific antibodies (gray areas marked by asterisks), display prominent postsynaptic densities (arrows), receiving presynaptic inputs from DAB$^-$ host cells (no stain). Error bars represent SEM.
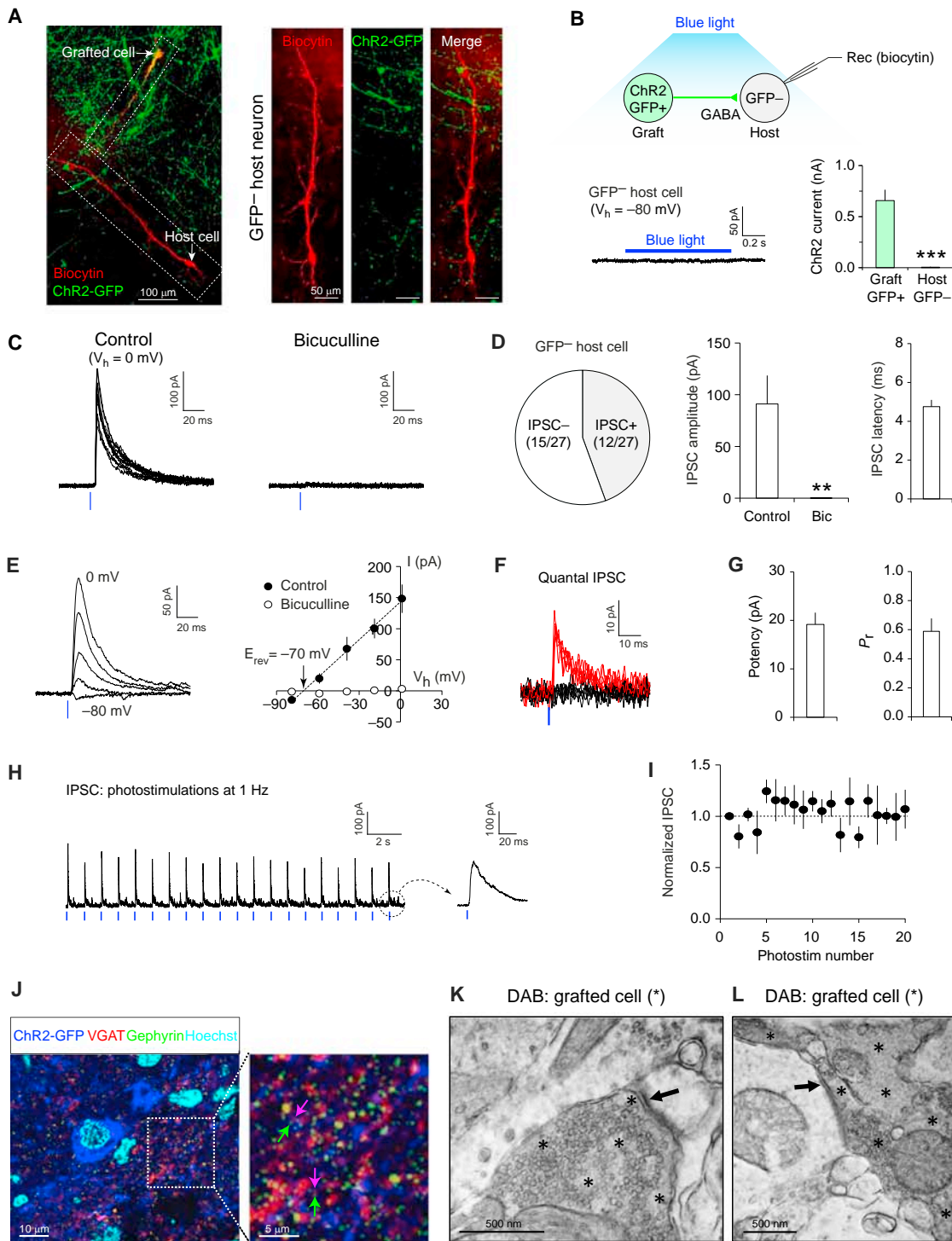
Figure 6. Optogenetic Stimulations of Transplanted Human mGINs Induce GABAergic Postsynaptic Responses in Host Hippocampal Neurons

(A) Left, a microscopic image showing both a GFP$^+$ grafted human MGE cell and a GFP$^-$ host pyramidal neuron in the CA3 of the hippocampus (dotted squares; cell bodies are indicated by arrows). These cells were labeled with biocytin-streptavidin with recording pipettes (red). The grafted cell sends out projections toward the host pyramidal neuron. Right, microscopic images showing the soma and dendrites of the same GFP$^-$ pyramidal neuron as in the left image. Projections from grafted human mGINs are shown in the middle (green, ChR2-GFP).

(B) Top, blue light illumination evokes AP firings in GFP$^+$ mGIN expressing ChR2 and induces the release of GABA at axon terminals, generating postsynaptic responses in the recorded GFP$^-$ host neuron. Bottom left, blue light illumination (0.61 mW/mm^2, blue horizontal bar) did not induce ChR2-mediated current in GFP$^-$ host neurons at −80 mV in voltage-clamp mode, indicating the lack of ChR2 expression. Bicuculline (30 μM) was added to inhibit GABAergic responses in

(legend continued on next page)

Induction of TLE in Nod-Scid Mice

The Animal Care and Use Committee at McLean Hospital approved all animal procedures. For induction of TLE, 7-week-old male and female Nod-Scid mice (Charles River Laboratory) were injected with 400 mg/kg Pilocarpine intraperitoneally (i.p.), 30 min after N-methylscopolamine bromide (1 mg/kg, i.p.) administration to reduce peripheral cholinergic effects (Mazzuferi et al., 2012). To limit the duration of status epilepticus (SE) and extent of damage in the hippocampus, diazepam (10 mg/kg) was injected ip 90 min after seizure induction. The severity of convulsive responses was monitored and classified according to the modified Racine scale (Shibley and Smith, 2002). Ten days after pilocarpine injection, mice that showed stage 3, 4, or 5 seizures were subject to 7 days of continuous video monitoring for SRS. Mice showing SRS with stage 3, 4, or 5 during the 7-day recording period were designated as TLE mice and were randomly assigned for subsequent transplantation and behavioral analysis. Detailed information can be found in the Supplemental Experimental Procedures.

Transplantation of Human MGE Cells into Hippocampus of TLE Model Mice

Differentiated and FACS-sorted human MGE cells were transplanted into TLE model mice at the following coordinates: AP-1.75 mm, L ± 2.3 mm, V −1.7 mm for the rostral CA3 site; AP-3.25 mm, L ± 3.0 mm, V −3.65 mm, −2.9 mm and −2.0 mm for the three caudal sites along the dorso-ventral axis of the hippocampus in this coronal plane. A total of 5×10^4 MGE cells in a 0.5 μl volume were delivered at each of the target coordinates. Sterile, stainless steel bone screw recording electrodes (diameter, 0.5mm; length, 1.1mm; Plastics One) soldered with a lead wire were placed epidurally through rostral burr holes in the skull (AP-1.75 mm, L +2.3 mm), and reference electrodes were positioned caudal to lambda. Electrodes were secured with a rapid-curing dental cement (DenMat Holdings). Detailed information is in the Supplemental Experimental Procedures.

Behavioral Analysis

Continuous Video EEG Recording of Transplanted Mice

Three months after transplantation, seizure activity of control or MGE-transplanted TLE mice was recorded with a MP150 Biopac data acquisition System, and EEG100C EEG amplifier module along with Eco Black Box security camera system (Lorex Technology). EEG seizures with high-frequency, high-voltage synchronized polyspike profiles with amplitudes greater than 2-fold that of background and a duration of greater than 15 s (Hunt et al., 2013) were analyzed with AcqKnowledge 4.0 EEG Acquisition and Reader Software

(BIOPAC Systems) by investigators who were blind to treatment conditions. This was followed by confirmation of EEG seizure activity by video recording.

Y Maze

We used a three-arm Y maze for this study: each arm was 3 cm wide, 40 cm in length, and had a wall height of 12 cm. Mice were initially placed within one arm, and the sequence and number of entries was recorded for each mouse over a 10 min period.

Novel Object Recognition Test

For a training session, each mouse was placed into an open-field box (42 × 42 × 31 cm) containing two identical objects and allowed to freely explore for 3 min. One hour after the training session, one of the familiar objects was replaced with a novel object (defined as the test session). The time that each animal spent exploring the novel object compared to the familiar object was recorded and traced with Ethovision software (Noldus).

Locomotion Test

The home cage (7 1⁄2 × 11 1⁄2 × 5 in) containing an individual mouse was placed in the center of a PAS monitoring frame (San Diego Instruments) with 4 × 8 photobeam configuration for 15 min under standard overhead lighting conditions. Total photobeam break numbers were detected by PAS software.

Handling Test

Aggressiveness of the mice was assessed as described previously (Hunt et al., 2013) with some modifications. Each of the following three tasks was performed for 15 s: (1) nonstressful handling (stroking slowly along the back of the mouse in the direction of the grain of fur), (2) stressful handling (vigorous stroking against the grain of the fur), and (3) pinching at the tail base with a rubber-ended forceps (Fine Science tools). Reaction to each handling was scored by investigators blinded to treatment conditions with the following rating scale: (1) initial struggle, but calmed within 15 s, (2) struggle for more than 15 s, (3) struggle for more than 15 s and exhibiting one or more defensive reactions (piloerection, flattening of the ears against the head, and attempt to bite or back away from the experimenter), and (4) struggled for more than 15 s and exhibited flight behavior (loud vocalization or wild running). Summation of these three scores provided a total aggressiveness score for each mouse.

More detailed information of behavioral analysis is in the Supplemental Experimental Procedures.

Immunohistochemistry, Cell Counting, and Statistical Analysis

Transplanted mice were terminally anesthetized with an i.p. overdose of pentobarbital (150 mg/kg, Sigma-Aldrich) and perfused transcardially with heparin saline (0.1% heparin in saline) followed by paraformaldehyde (4%)

---

the recorded host neuron. Bottom right, the comparison of ChR2 currents between grafted and host cells (n = 25 and 27 cells, respectively), which received the same blue light illumination (0.61 mW/mm^2). ***p < 0.001.

(C) Left, representative traces of postsynaptic currents recorded in a GFP$^−$ host neuron. Postsynaptic responses were recorded at 0 mV in voltage-clamp mode and induced by photostimulations at 12.5 mW/mm^2 (1 ms duration, blue vertical line). Blue light illumination was applied every 10 s. Right, these postsynaptic currents were completely inhibited by the application of GABA$_A$ receptor antagonist bicuculline (30 μM) in the same neuron.

(D) Left, 44% of total 27 GFP$^−$ host neurons displayed GABA$_A$ receptor-mediated inhibitory postsynaptic currents (IPSC) induced by photostimulations. Middle, a summary graph showing the average amplitude of IPSCs before and after the application of bicuculline as in (c). **p < 0.01. Right, a plot showing the average synaptic latency of IPSCs induced optogenetically and recorded in GFP$^−$ host neurons (n = 10 neurons). The synaptic latency was quantified as the time interval between the start of photostimulations and the onset of synaptic responses.

(E) Left, representative traces of postsynaptic currents recorded in a GFP$^−$ host neuron. Postsynaptic currents were induced by blue light illuminations at 12.5 mW/mm^2 (1 ms duration, blue vertical line) and recorded in voltage-clamp mode at –80, –60, –40, –20, and 0 mV. Right, a current-voltage plot of the postsynaptic responses. Peak amplitudes of postsynaptic currents were plotted versus holding potential (V$_h$, closed circles). Linear regression (a dotted line) reveals the reversal potential of the postsynaptic currents (E$_{rev}$ = – 70 mV). The application of 30 μM bicuculline inhibited postsynaptic currents completely at all holding potentials examined (open circles). n = 3 neurons.

(F) Overlaid traces of quantal IPSCs (qIPSCs) indicate both successes (red traces) and failures (black traces). qIPSCs were induced by blue light illuminations (blue vertical line) and recorded in GFP$^−$ host neurons as in (C).

(G) Summary plots showing the average potency (quantal size) and release probability (P_r) of qIPSCs. n = 6 neurons.

(H) A representative trace of IPSCs induced by train photostimulations. IPSCs were induced by blue light illumination applied at 1 Hz (12.5 mW/mm^2, 1 ms duration, blue vertical lines) and recorded in GFP$^−$ host neurons at 0 mV in voltage-clamp mode. A trace on the right indicates the last evoked iPSC (a dotted circle).

(I) A summary plot of IPSCs during 1 Hz train photostimulations as in (H). The peak amplitude of iPSCs was normalized to the first iPSC (a dotted line; n = 3).

(J) Immunohistochemistry analysis of transplanted human mGINs. Hoechst (sky blue) was used as nuclear counterstain. Arrows in magenta indicate GABAergic presynaptic terminals of GFP$^+$ grafted cells (double-stained with ChR2-GFP and VGAT), and green arrows indicate inhibitory postsynaptic densities (stained with gephyrin, green) of GFP$^−$ cells.

(K and L) TEM images of grafted cells stained with DAB for human-cytoplasm-specific antibodies (gray areas are marked by asterisks). DAB$^−$ host cells (no stain) receives synaptic inputs (arrows) from DAB$^+$ grafted cells. Error bars represent SEM.
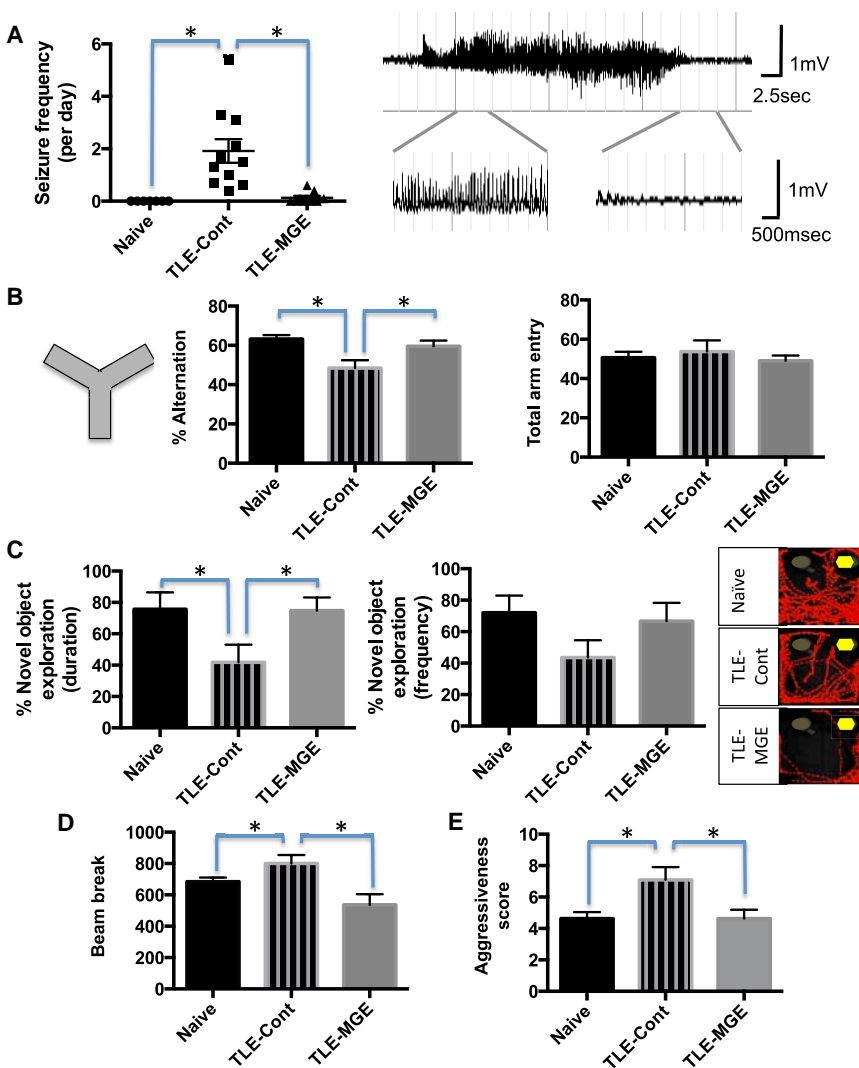
Figure 7. Transplanted mGINs Reduce Seizure Activity and Other Behavioral Abnormalities

(A) Video-EEG analysis of naive mice (n = 6), vehicle-injected control TLE mice (TLE-Cont, n = 11), and MGE-transplanted TLE mice (TLE-MGE, n = 9). Right, representative seizure EEG activity with high-frequency, high-voltage synchronized polyspikes.

(B) Y maze test of naive mice (n = 9), vehicle-injected TLE control mice (n = 10), and transplanted TLE (n = 8), shown by the percentage of alternation as an indicative of short-term memory and by the number of total arm entry as an indicative of locomotor activity.

(C) Novel object recognition test of naive mice (n = 12), vehicle-injected TLE control mice (n = 11), and transplanted TLE mice (n = 8), shown by the percentage of time spent near a novel object to total time spent exploring either object (duration), and by the percentage of number of visits near novel object to total number of visits exploring objects (frequency). Right, representative tracing of mouse center point during trial detected with Ethovision software. Novel object is shown as a yellow hexagonal symbol.

(D) Locomotion test of naive mice (n = 14), vehicle-injected control TLE mice (n = 11) and MGE-transplanted TLE mice (n = 8), as shown by the number of photobeam breaks in 15 min.

(E) Handling test of naive mice (n = 15), vehicle-injected TLE control mice (n = 11), and transplanted TLE mice (n = 10).

Data are presented as the average ± SEM. *p < 0.05, ANOVA followed by post hoc analysis with nonparametric Kruskal-Wallis test in (A) and by post hoc analysis with Fisher's LSD in (B–E). See also Figure S7.

2 weeks or 4 months postgrafting. Brains were removed, postfixed in 4% paraformaldehyde for 12 hr, equilibrated in 20% sucrose/PBS solution, and then sectioned coronally at 40 μm with a freezing microtome. Histological analysis was performed as described previously (Kim et al., 2014), and detailed information is in the Supplemental Experimental Procedures.

Transmission Electron Microscopy

See the Supplemental Experimental Procedures for details.

Statistical Analysis

For statistical analysis, we performed a Student's t test (α = 0.05) for comparison of two groups with Prism6 software (Graph Pad). For multiple sample comparison, we performed ANOVA with an α level of 0.05 in order to determine possible statistical differences between group means. When significant differences were found, post hoc analysis was performed with Fisher's least significant difference (α = 0.05) again with the use of Prism6 software. For samples with unequal variances, a nonparametric Kruskal-Wallis test was performed with Prism6 software.

Electrophysiology, Optogenetic Stimulations, and Neurolucida Tracing

For electrophysiological studies, MGE cells were infected with lentivirus that express ChR2 (H134R)-GFP fusion protein under the control of synapsin promoter (University of Pennsylvania Vector Core) at day 14 of differentiation.

Transduction efficiency was 26.3% ± 4.7% (n = 4). The cells underwent FACS and were transplanted as described above. Two to five months after transplantation, acute brain slices containing the hippocampus were prepared using a vibrating microtome for electrophysiological analysis. After recovery, brain slices were placed in the recording chamber and continuously perfused at the rate of 1 ml per min with the artificial cerebrospinal fluid containing 130 mM NaCl, 2.5 mM KCl, 2.5 mM CaCl₂, 1 mM MgSO₄, 1.25 mM NaH₂PO₄, 26 mM NaHCO₃, and 10 mM glucose with 95% O₂ and 5% CO₂. Whole-cell patch-clamp recordings were performed at 31°–33°C with EPC-9 amplifier and Pulse v8.8 software (HEKA Elektronik). For recording grafted MGE-derived neurons (GFP⁺ cells) and host hippocampal interneurons, the patch electrodes (~5 MOhm resistance) were filled with solution containing 150 mM K-gluconate, 5 mM NaCl, 1 mM MgCl₂, 10 mM HEPES, 0.2 EGTA, 2 mM MgATP, 0.5 mM NaGTP, and 5 mM biocytin (290 mOsm, adjusted to pH 7.3 with potassium hydroxide). For recording GFP⁻ host hippocampal neurons, the patch electrodes were filled with solution containing 140 mM Cs-methanesulfonate, 5 mM NaCl, 1 mM MgCl₂, 10 mM HEPES, 0.2 EGTA, 2 mM MgATP, 0.5 mM NaGTP, 5 mM QX 314 chloride, and 5 mM biocytin (290 mOsm, adjusted to pH 7.3 with caesium hydroxide). Liquid junction potential of 15.5 and 8.9 mV was corrected for the K-gluconate- and caesium-based pipette solutions, respectively. Series (access) resistance was not compensated. Blue collimated light-emitting diode (LED) with 470 nm peak wavelength (M470L2, Thorlabs) was used for photostimulations of grafted MGE-derived cells expressing ChR2-GFP. Brain slices in the recording chamber were illuminated through a 40× water-immersion objective lens (IR-Achroplan, Carl Zeiss). Illumination area was 0.26 mm² and was centered at the cell patched for recording.

Offline data analysis was performed with Clampfit 9 (Molecular Devices). Reagents were purchased from Tocris Bioscience (QX 314 chloride, biocytin, and NBQX) or Sigma-Aldrich (ATP, GTP, and bicuculline methochloride). For statistical analyses of electrophysiological data, we used ANOVA with Bonferroni's simultaneous multiple comparisons. Statistical analysis was performed with Minitab16 (Minitab), and $p < 0.05$ was considered statistically significant.

After electrophysiological recordings, brain slices were fixed in 4% paraformaldehyde at $4°C$ overnight. Recorded cells loaded with biocytin were labeled with streptavidin, Alexa 568 conjugate (20 μg/ml in PBS, Molecular Probes) as described previously (Cho et al., 2013). Images of biocytin-loaded and streptavidin-labeled cells were taken with z stack function with a Leica TSC SP8 confocal microscope. The confocal images were then used for neuron tracing with Neurolucida software (Microbright Field).

Single-Cell RT-PCR
See the Supplemental Experimental Procedures for details.

SUPPLEMENTAL INFORMATION

Supplemental Information contains Supplemental Experimental Procedures, seven figures, and two movies and can be found with this article online at http://dx.doi.org/10.1016/j.stem.2014.10.006.

AUTHOR CONTRIBUTIONS

ACKNOWLEDGMENTS

REFERENCES

Baraban, S.C., Southwell, D.G., Estrada, R.C., Jones, D.L., Sebe, J.Y., Alfaro-Cervello, C., García-Verdugo, J.M., Rubenstein, J.L., and Alvarez-Buylla, A. (2009). Reduction of seizures by transplantation of cortical GABAergic interneuron precursors into Kv1.1 mutant mice. Proc. Natl. Acad. Sci. USA 106, 15472–15477.

Bjarkam, C.R., Glud, A.N., Margolin, L., Reinhart, K., Franklin, R., Deding, D., Ettrup, K.S., Fitting, L.M., Nielsen, M.S., Sørensen, J.C., and Cunningham, M.G. (2010). Safety and function of a new clinical intracerebral microinjection instrument for stem cells and therapeutics examined in the Göttingen minipig. Stereotact. Funct. Neurosurg. 88, 56–63.

Brooks-Kayal, A.R., Bath, K.G., Berg, A.T., Galanopoulou, A.S., Holmes, G.L., Jensen, F.E., Kanner, A.M., O'Brien, T.J., Whittemore, V.H., Winawer, M.R., et al. (2013). Issues related to symptomatic and disease-modifying treatments affecting cognitive and neuropsychiatric comorbidities of epilepsy. Epilepsia 54 (Suppl 4), 44–60.

Chen, K.G., Mallon, B.S., McKay, R.D., and Robey, P.G. (2014). Human pluripotent stem cell culture: considerations for maintenance, expansion, and therapeutics. Cell Stem Cell 14, 13–26.

Cho, J.H., Deisseroth, K., and Bolshakov, V.Y. (2013). Synaptic encoding of fear extinction in mPFC-amygdala circuits. Neuron 80, 1491–1507.

Christoph, C.H. (2008). Temporal lobe resection–does the prospect of seizure freedom outweigh the cognitive risks? Nat Clin Pract Neurol 4, 66–67.

Cossart, R., Dinocourt, C., Hirsch, J.C., Merchan-Perez, A., De Felipe, J., Ben-Ari, Y., Esclapez, M., and Bernard, C. (2001). Dendritic but not somatic GABAergic inhibition is decreased in experimental epilepsy. Nat. Neurosci. 4, 52–62.

Cramer, J.A., Mintzer, S., Wheless, J., and Mattson, R.H. (2010). Adverse effects of antiepileptic drugs: a brief overview of important issues. Expert Rev. Neurother. 10, 885–891.

Curia, G., Longo, D., Biagini, G., Jones, R.S., and Avoli, M. (2008). The pilocarpine model of temporal lobe epilepsy. J. Neurosci. Methods 172, 143–157.

de Lanerolle, N.C., Kim, J.H., Robbins, R.J., and Spencer, D.D. (1989). Hippocampal interneuron loss and plasticity in human temporal lobe epilepsy. Brain Res. 495, 387–395.

Doischer, D., Hosp, J.A., Yanagawa, Y., Obata, K., Jonas, P., Vida, I., and Bartos, M. (2008). Postnatal differentiation of basket cells from slow to fast signaling devices. J. Neurosci. 28, 12956–12968.

Engel, J. (2002). Epilepsy in the world today: medical point of view. Epilepsia 43 (Suppl 6), 12–13.

Engel, J., Jr.; International League Against Epilepsy (ILAE) (2001). A proposed diagnostic scheme for people with epileptic seizures and with epilepsy: report of the ILAE Task Force on Classification and Terminology. Epilepsia 42, 796–803.

Fine, A., Meldrum, B.S., and Patel, S. (1990). Modulation of experimentally induced epilepsy by intracerebral grafts of fetal GABAergic neurons. Neuropsychologia 28, 627–634.

Gröticke, I., Hoffmann, K., and Löscher, W. (2007). Behavioral alterations in the pilocarpine model of temporal lobe epilepsy in mice. Exp. Neurol. 207, 329–349.

Hattiangady, B., Rao, M.S., and Shetty, A.K. (2008). Grafting of striatal precursor cells into hippocampus shortly after status epilepticus restrains chronic temporal lobe epilepsy. Exp. Neurol. 212, 468–481.

Hirsch, J.C., Agassandian, C., Merchán-Pérez, A., Ben-Ari, Y., DeFelipe, J., Esclapez, M., and Bernard, C. (1999). Deficit of quantal release of GABA in experimental models of temporal lobe epilepsy. Nat. Neurosci. 2, 499–500.

Hunt, R.F., Girskis, K.M., Rubenstein, J.L., Alvarez-Buylla, A., and Baraban, S.C. (2013). GABA progenitors grafted into the adult epileptic brain control seizures and abnormal behavior. Nat. Neurosci. 16, 692–697.

Jensen, F.E. (2014). Epilepsy in 2013: progress across the spectrum of epilepsy research. Nat Rev Neurol 10, 63–64.

Kim, T.-G., Yao, R., Monnell, T., Cho, J.-H., Vasudevan, A., Koh, A., Peeyush, K.T., Moon, M., Datta, D., Bolshakov, V.Y., et al. (2014). Efficient specification of interneurons from human pluripotent stem cells by dorsoventral and rostrocaudal modulation. Stem Cells 32, 1789–1804.

Kobayashi, M., and Buckmaster, P.S. (2003). Reduced inhibition of dentate granule cells in a model of temporal lobe epilepsy. J. Neurosci. 23, 2440–2452.

Le Magueresse, C., and Monyer, H. (2013). GABAergic interneurons shape the functional maturation of the cortex. Neuron 77, 388–405.

Lindvall, O., and Björklund, A. (1992). Intracerebral grafting of inhibitory neurons. A new strategy for seizure suppression in the central nervous system. Adv. Neurol. 57, 561–569.

Löscher, W., Ebert, U., Lehmann, H., Rosenthal, C., and Nikkhah, G. (1998). Seizure suppression in kindling epilepsy by grafts of fetal GABAergic neurons in rat substantia nigra. J. Neurosci. Res. 51, 196–209.

Maisano, X., Litvina, E., Tagliatela, S., Aaron, G.B., Grabel, L.B., and Naegele, J.R. (2012). Differentiation and functional incorporation of embryonic stem cell-derived GABAergic interneurons in the dentate gyrus of mice with temporal lobe epilepsy. J. Neurosci. 32, 46–61.

Mallon, B.S., Chenoweth, J.G., Johnson, K.R., Hamilton, R.S., Tesar, P.J., Yavatkar, A.S., Tyson, L.J., Park, K., Chen, K.G., Fann, Y.C., and McKay, R.D. (2013). StemCellDB: the human pluripotent stem cell database at the National Institutes of Health. Stem Cell Res. (Amst.) 10, 57–66.

Marco, P., Sola, R.G., Pulido, P., Alijarde, M.T., Sánchez, A., Ramón y Cajal, S., and DeFelipe, J. (1996). Inhibitory neurons in the human epileptogenic temporal neocortex. An immunocytochemical study. Brain *119*, 1327–1347.

Mazzuferi, M., Kumar, G., Rospo, C., and Kaminski, R.M. (2012). Rapid epileptogenesis in the mouse pilocarpine model: video-EEG, pharmacokinetic and histopathological characterization. Exp. Neurol. *238*, 156–167.

Müller, C.J., Gröticke, I., Bankstahl, M., and Löscher, W. (2009). Behavioral and cognitive alterations, spontaneous seizures, and neuropathology developing after a pilocarpine-induced status epilepticus in C57BL/6 mice. Exp. Neurol. *219*, 284–297.

Nicholas, C.R., Chen, J., Tang, Y., Southwell, D.G., Chalmers, N., Vogt, D., Arnold, C.M., Chen, Y.J., Stanley, E.G., Elefanty, A.G., et al. (2013). Functional maturation of hPSC-derived forebrain interneurons requires an extended timeline and mimics human neural development. Cell Stem Cell *12*, 573–586.

Okaty, B.W., Miller, M.N., Sugino, K., Hempel, C.M., and Nelson, S.B. (2009). Transcriptional and electrophysiological maturation of neocortical fast-spiking GABAergic interneurons. J. Neurosci. *29*, 7040–7052.

Rice, A.C., Floyd, C.L., Lyeth, B.G., Hamm, R.J., and DeLorenzo, R.J. (1998). Status epilepticus causes long-term NMDA receptor-dependent behavioral changes and cognitive deficits. Epilepsia *39*, 1148–1157.

Shibley, H., and Smith, B.N. (2002). Pilocarpine-induced status epilepticus results in mossy fiber sprouting and spontaneous seizures in C57BL/6 and CD-1 mice. Epilepsy Res. *49*, 109–120.

Southwell, D.G., Froemke, R.C., Alvarez-Buylla, A., Stryker, M.P., and Gandhi, S.P. (2010). Cortical plasticity induced by inhibitory neuron transplantation. Science *327*, 1145–1148.

Southwell, D.G., Nicholas, C.R., Basbaum, A.I., Stryker, M.P., Kriegstein, A.R., Rubenstein, J.L., and Alvarez-Buylla, A. (2014). Interneurons from embryonic development to cell-based therapy. Science *344*, 1240622.

Spreafico, R., Battaglia, G., Arcelli, P., Andermann, F., Dubeau, F., Palmini, A., Olivier, A., Villemure, J.G., Tampieri, D., Avanzini, G., and Avoli, M. (1998). Cortical dysplasia: an immunocytochemical study of three patients. Neurology *50*, 27–36.

Walia, K.S., Khan, E.A., Ko, D.H., Raza, S.S., and Khan, Y.N. (2004). Side effects of antiepileptics—a review. Pain Pract. *4*, 194–203.

Wieser, H.G.; ILAE Commission on Neurosurgery of Epilepsy (2004). ILAE Commission Report. Mesial temporal lobe epilepsy with hippocampal sclerosis. Epilepsia *45*, 695–714.

Yu, D.X., Marchetto, M.C., and Gage, F.H. (2013). Therapeutic translation of iPSCs for treating neurological disease. Cell Stem Cell *12*, 678–688.